Structural Characterization of Membrane Insertion of M13 Procoat, M13 Coat, and Pf3 Coat Proteins†

E. Thiaudière,‡ M. Soekarjo,‡ E. Kuchinka,‡,§ A. Kuhn,§ and H. Vogel*,‡

Institute of Physical Chemistry, Swiss Federal Institute of Technology, CH-1015 Lausanne, Switzerland, and Institute of Microbiology, University of Karlsruhe, Kaiserstrasse 12, D-7500 Karlsruhe, FRG

Received June 10, 1993; Revised Manuscript Received August 30, 1993®

ABSTRACT: A new, simple, and efficient purification method has been developed for the extremely hydrophobic M13 procoat, M13 coat, and Pf3 coat proteins. Homogeneous preparations were obtained in 2-propanol/0.1% TFA, where M13 coat protein is found to be dissolved in a monomeric form, and the two other proteins as dimers or trimers. The conformations of these particular proteins in different environments have been determined by circular dichroism and infrared spectroscopy. In organic solvents, the proteins adopt a conformation with an average helix content of 90%. In lipid bilayers composed of phosphatidylcholine and phosphatidylglycerol lipids, the average helix content is 50% for M13 procoat protein, 60% for M13 coat protein, and 75% for Pf3 coat protein. The orientational order parameter S_α of the protein helices in planar lipid bilayers have been determined by polarized infrared measurements in the amide I spectral range. The helices of the three proteins are oriented preferentially parallel to the membrane normal, with $S_\alpha = 0.63$ for M13 procoat protein, $S_\alpha = 0.58$ for Pf3 coat protein, and a distinctly higher value of $S_\alpha = 0.81$ for M13 coat protein.

Protein integration in or translocation across membranes is a fundamental process in procaryotic and eucaryotic cells. The biosynthesis of almost all cellular proteins begins in the cytoplasm. During or after synthesis, noncytoplasmic proteins are targeted to an appropriate organelle, thereby either inserting into or crossing one or several membranes. Newly synthesized secreted or integral membrane proteins carry specific regions (designated as leader, signal, or stop–transfer sequences) that play a functional role in the membrane insertion/transfer process. In eucaryotic cells, protein synthesis and membrane transport are often synchronously linked by a complicated signal–receptor mechanism (Rapoport, 1992; Nunnari & Walter, 1992). However, small proteins insert into membranes independently of complex translocation machineries (Wolfe et al., 1985; Rohrer & Kuhn, 1990; Wiech et al., 1987). This suggests that such small proteins must have the structural properties necessary for targeting and translocation within their primary amino acid sequence. Here we focus on the membrane insertion of two coat proteins of the filamentous bacteriophages M13 and Pf3. *Escherichia coli* M13 and *Pseudomonas aeruginosa* phage Pf3 coat proteins insert into the bacterial cytoplasmic membrane prior to their assembly into viral particles. Both proteins are similar in length (50 and 44 residues, respectively) but do not share any sequence homology. As schematically shown in Figure 1, both coat proteins contain a hydrophobic region of about 20 amino acid residues, flanked by an acidic amino-terminal region and a basic segment at the carboxy terminus. The acidic regions of both proteins are located in the periplasm, whereas the basic regions remain in the cytoplasm [for a review, see Kuhn and Troschel (1992)].

Notwithstanding these similarities, the membrane insertion processes of the two coat proteins differ considerably. The M13 coat protein is synthesized in *E. coli* cells as a precursor, procoat protein, with a 23-residue leader sequence at its N-terminus (Figure 1). After synthesis, procoat binds to the inner surface of the plasma membrane and subsequently translocates as a loop structure across the membrane in the presence of a transmembrane electrical potential (Gallusser & Kuhn, 1990; Kuhn, 1987; Kuhn et al., 1986). In this configuration, procoat is cleaved by leader peptidase, yielding the transmembrane coat protein and a leader peptide. As opposed to M13 coat protein, Pf3 coat protein is synthesized without a leader sequence at its amino terminus and directly transfers its amino terminus across the membrane (Kuhn et al., 1990). Moreover, it was shown that only M13 procoat but not M13 coat protein inserts into the *E. coli* membrane *in vivo* (Rohrer & Kuhn, 1990).

It was also shown that the insertion of M13 procoat protein can be reconstituted into phospholipid vesicles *in vitro* (Ohno-Iwashita & Wickner, 1983; Geller & Wickner, 1985). This opens the way to investigation of the structural requirements of proteins for insertion into a lipid bilayer. To understand how this process occurs, we describe in the present paper the structure determination of the M13 procoat, M13 coat, and Pf3 coat proteins (secondary structure, membrane orientation, state of aggregation) in different environments by applying circular dichroism (CD)[1] and Fourier-transform infrared (FTIR) spectroscopy.

To address questions concerning the protein structure, we developed a new, simple, and efficient purification method

† This work was supported by grants from the European Community (Science Plan, SCCX-CT90-0025 to A.K. and H.V.) and from the Swiss National Science Foundation (FN 31-27910.89 to H.V.). E.K. was partly supported by a short-term fellowship from the European Molecular Biology Organization.

* Address correspondence to this author.
‡ Swiss Federal Institute of Technology.
§ University of Karlsruhe.

® Abstract published in *Advance ACS Abstracts,* November 1, 1993.

[1] Abbreviations: ATR, attenuated total reflection; CD, circular dichroism; EDTA, ethylenediaminetetraacetic acid; FTIR, Fourier-transform infrared; POPC, 1-palmitoyl-2-oleoyl-*sn*-3-phosphatidylcholine; POPG, 1-palmitoyl-2-oleoyl-*sn*-3-phosphatidylglycerol; SDS–PAGE, sodium dodecyl sulfate–polyacrylamide gel electrophoresis; SUV, small unilamellar vesicle(s); TFA, trifluoroacetic acid; *r*, lipid to protein molar ratio; R_{ATR}, ATR dichroic ratio.

0006-2960/93/0432-12186$04.00/0

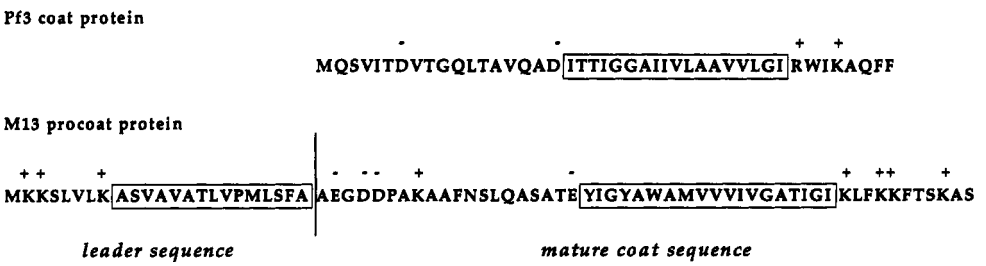

FIGURE 1: Amino acid sequences of M13 procoat and Pf3 coat proteins. The arrow indicates the cleavage site of procoat protein by leader peptidase between the leader sequence from amino acids −23 to −1 and the mature coat protein sequence from 1 to 50. The charged amino acids are indicated; the rectangles symbolize the hydrophobic, putative transmembrane domains. The H5 procoat mutant protein used in the present work contains a single amino acid mutation at sequence position −3 with an exchange of Ser to Phe.

for the various proteins. Previously, M13 procoat protein had been partially purified (75% purity) in SDS (Zwizinski & Wickner, 1982). These authors were able to isolate the protein from M13 amber 7-infected cells because in this mutant phage there is a pronounced delay in the processing of procoat protein to coat protein. Sodium dodecyl sulfate, however, shows many drawbacks for reconstitution experiments, because it is difficult to remove from the membrane preparations. In the present work, we report on an improved isolation procedure that omits detergent. A procoat protein mutant, termed H5, which is not cleaved by leader peptidase, was used. The mutation substitutes Ser at position −3 by Phe, which does not affect the membrane translocation pathway of this protein (Kuhn & Wickner, 1985). The purification protocols yielded the procoat protein in organic solvents in a dimeric form, suitable for biophysical studies. Furthermore, the coat proteins could be extracted from whole phages by an extraction procedure with 2-propanol, obtaining molecularly dissolved proteins. The secondary structures of these proteins were investigated in organic and aqueous solutions, and in lipid membrane preparations by CD and FTIR spectroscopy. Both methods allow for protein secondary structure determination [for reviews, see Surewicz and Mantsch (1988) and Johnson (1988)]. CD measurements are known to yield in general quite reliable data on the average α-helix content of proteins, but report with less confidence on β-structures and β-turns. On the other hand, the protein secondary structure can be determined from the amide I band of an infrared spectrum with reliable results for the different secondary structure elements such as α-helices, β-strands, turns, and nonregular features, but an uncertainty arises due to the spectral contribution of water in the case of aqueous preparations. We therefore gathered complementary structural data for the proteins under investigation by using both spectroscopic methods. Furthermore, FTIR measurements were performed by the ATR technique on planar protein/lipid multilayers supported on solid Ge substrates in order to determine the orientational distribution of the different secondary structural motifs of the proteins in the lipid bilayer. This technique has previously been applied quite successfully for determining the orientational distribution of lipids, proteins, and polypeptides in planar lipid bilayers (Vogel et al., 1983; Blume et al., 1988; Gremlich et al., 1983; Kleffel et al., 1985; Fringeli et al., 1986; Cornell et al., 1989; Frey & Tamm, 1991).

MATERIALS AND METHODS

Materials. The lipids 1-palmitoyl-2-oleoylphosphatidylcholine (POPC) and 1-palmitoyl-2-oleoylphosphatidylglycerol (POPG) were from Avanti Polar Lipids; all other chemicals were from Fluka and of the best quality available. Reference proteins for secondary structure evaluation of IR spectra were from Sigma Chemicals (Eugene, OR). They comprised hemoglobin, myoglobin, papain, prealbumin, cytochrome *c*, alcohol dehydrogenase, concanavalin A, lysozyme, pepsin, protease, chymotrypsin, and triosephosphate isomerase.

Bacterial Strains and Plasmids. *E. coli* HJM 114 (Δ *lacpro*) F′ (*lacpro*) and *Pseudomonas aeruginosa* were used to grow M13 and Pf3 phage, respectively. *E. coli* LC 137 (htpR, lon, lac_{am}, trp_{am}, pho_{am}, mal_{am}, rpsL, $svpC^{ts}$, tsc:Tn10) was used for procoat expression. Gene VIII of M13 coding for the H5 procoat mutant was in the pJF119 HE plasmid (Fürste et al., 1986; Kuhn et al., 1990) under the control of an inducible tac promotor, termed pJQ-8-H5.

Isolation and Purification of M13 and Pf3 Coat Proteins. M13 and Pf3 phages were grown and isolated according to published procedures (Wickner, 1975; Thomas & Day, 1981). Phages were stored as a stable suspension in 0.1 M Tris-HCl (pH 7)/0.1% NaN_3 at 4 °C. Aliquots of phage suspension in buffer were vortexed with an equal volume of chloroform, yielding a white precipitate of phages. After centrifugation for 15 min at 20000*g* (Centrikon T-124, rotor A8-24, Kontron), the phages form a pellet at the water/chloroform interface. The pellet was resuspended in water, again vortexed with chloroform, and centrifuged. This washing step was repeated 5 times. The ultimate pellet was dissolved in an appropriate amount of 2-propanol containing 0.1% TFA (v/v), yielding a 100 μM–2 mM solution of the coat protein, which was isolated as the supernatant of a final centrifugation step, leaving the DNA as a clear pellet. The extract was purified once by HPLC on a Hewlett Packard Series 1050 instrument over a Nucleosyl 100-7 C2 reversed-phase column (Macherey-Nagel, Düren, Germany) using a water/2-propanol gradient in 0.1% TFA. The major peak of the particular coat protein was collected, showing an UV absorbance spectrum with an absorption ratio (280 nm to 260 nm) of 1.8. The purity of the coat proteins was assessed by SDS–PAGE (Ito et al., 1980). A single protein band was observed after silver staining of the gels in each case. The bands of M13 coat protein were identified by Western blots using polyclonal antibodies to M13 coat and the Amersham ECL kit (Beaconsfield, U.K.) as the detection system.

Isolation and Purification of M13 Procoat Protein. *E. coli* LC 137 with plasmid pJQ8-H5 was grown at 30 °C to 4×10^8 cells/mL in 2-L shaking cultures. IPTG was added at 0.5 mM, and the culture was continued for 4 h under extensive shaking. The cells were then chilled, and 200 mL of a 50 mM NaOH solution was added. After lysis, the cells were collected by centrifugation at 2000*g* for 20 min and resuspended in 50 mM Tris-HCl, pH 6.8. After sonication at 4 °C for 1 min, the membrane fragments were collected by centrifugation and subsequently sonicated at 4 °C for 1 min in order to homogenize the membranes. Membrane fragments were isolated by centrifugation at 20000*g*, followed twice by resuspension in water and centrifugation. The isolated

membranes were then stored at −50 °C prior to protein extraction. After being thawed, the membranes were washed once with ethanol and then extracted twice with formic acid/ethanol/2-propanol, 2/1/1 (v/v). The combined extracts were purified twice by HPLC on a Hewlett Packard Series 1050 instrument over a Nucleosyl 100-7 C2 reversed-phase column (Macherey-Nagel) using a water/2-propanol gradient in 0.1% TFA. The collected peaks were concentrated by ultrafiltration on Millipore Ultrafree-CL low binding cellulose (5000 NMWL) to a final concentration of 10–20 μM as determined by the UV absorbance at 280 nm (see below). SDS–PAGE and Western blots were made to monitor the amount and purity of the protein as described for M13 coat protein (see above). Total amino acid analysis and N-terminal amino acid sequencing of the isolated procoat protein sample were kindly performed by Dr. Stefan Stefanovic (Institute for Organic Chemistry, University of Tübingen, Germany). Determined molar ratios of amino acid residues were in accordance with those expected from the sequence.

Sample Preparation for Circular Dichroism Measurements. Peptide concentrations were determined by the UV absorbance at 280 nm using $\epsilon = 8000\ M^{-1}\ cm^{-1}$ for M13 procoat and coat proteins, and $6000\ M^{-1}\ cm^{-1}$ for Pf3 coat protein. Peptides were incorporated into vesicles using the following methods. If not otherwise stated, the buffer used for sample preparation was 1 mM Tris-HCl (pH 7.4)/0.1 mM EDTA.

"Mixed Film": Appropriate volumes of solutions of lipids [2 mM in chloroform/methanol, 1:1 (v/v)] and peptides in organic solvent were mixed. The solvent was evaporated first under a continuous flow of N_2 and then under vacuum. The resulting films were rehydrated with buffer and sonicated until a clear suspension of small unilamellar vesicles (SUV) was obtained. Finally, the samples were degassed with He.

"Preformed Vesicles": SUV were formed by sonication in buffer. Peptides in organic solvent were injected to a suspension of these vesicles under stirring. The final amount of organic solvent in the samples was smaller than 0.2% before the samples were degassed with He.

Circular Dichroism Measurements. Circular dichroism experiments were performed on an AVIV Model 62DS circular dichroism spectrometer (Lakewood, NJ). Unless otherwise stated, spectra between 186 and 250 nm of degassed, stirred 1 μM peptide solutions were acquired in quartz cuvettes of 0.01-, 0.1-, or 1-cm path length, at 25 °C. Blanks (organic solvent, buffer with or without lipids) were routinely recorded and subtracted from the original spectra. Buffer was 1 mM Tris-HCl (pH 7.4)/0.1 mM EDTA. In order to determine the secondary structure of a protein, the corresponding spectrum was fitted between 186 and 250 nm according to a modified procedure of Hennesy and Johnson (1981) as already described (Vogel, 1987).

Infrared Spectroscopy. FTIR measurements were performed using a Bomem Model 110 Michelson interferometer (Montreal, Canada) at a resolution of 4 cm^{-1}, equipped with a narrow-band, liquid N_2 cooled HgCdTe detector. For each experiment, 200–1000 scans were accumulated, Fourier-transformed, and triangularly apodized. Some spectra were splined with a third-order polynomial up to a degradation factor of 4. For attenuated total reflection (ATR) experiments, we used an overhead ATR unit (Specac, Kent, England) made with a trapezoidal-shaped germanium crystal (50 × 10 × 3 mm^3), an angle of incidence of 45° (Figure 2), and a grid polarizer of KRS5. Spectra of the plain ATR crystal were recorded for each polarization and subtracted from the respective membrane spectra. The germanium plate was

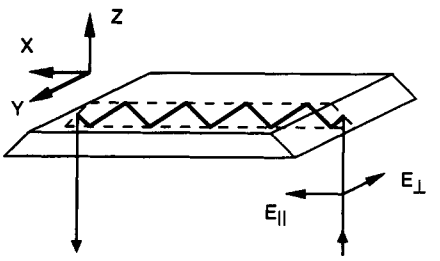

FIGURE 2: Schematic representation of the ATR-crystal used for polarized infrared measurements of planar lipid bilayers. $\mathbf{E}_\parallel$ and $\mathbf{E}_\perp$ define the electric field vectors of the incident polarized light. The coordinate system on the left define the orientations of the electric field vectors $\mathbf{E}_x$, $\mathbf{E}_y$, and $\mathbf{E}_z$ of the evanescent light wave in the supported, planar lipid film.

cleaned with chloroform/methanol, 1/1 (v/v). Planar multilamellar lipid membranes with or without peptides were spread from organic solvent on the crystal. Typically, 5 μg of peptide was used and mixed with the corresponding amount of lipid for a defined lipid-to-protein molar ratio, r. This corresponds to an average number of bilayers of 1 and 25 for $r = 2$ and 50, respectively.

Three different sample preparations were used: dry peptide/lipid films; the same films under a saturated D_2O vapor atmosphere; and films that were hydrated directly with D_2O. Transmittance spectra were calculated against blanks (germanium plate with or without D_2O).

Quantitative analysis of the polarized ATR spectra was performed as described by Fringeli and Günthard (1981). The dichroic ratio is defined as the ratio of the absorption polarized parallel to the plane of incidence, $A_\parallel$, to that polarized perpendicular, $A_\perp$, as $R_{ATR} = A_\parallel/A_\perp$. For an axially-symmetric molecule with an axially-symmetric distribution of the molecular director around the membrane normal by an angle Θ, the orientational order parameter of the molecular director is defined as $S_{mol} = \langle 3\cos^2\Theta - 1\rangle/2$, describing the space and time-averaged fluctuations of the molecular director around the membrane normal. Unfortunately, S_{mol} is experimentally not directly accessible. Only the orientational order parameter S_v of a particular vibrational transition moment M can be determined from the dichroic ratio of the corresponding spectral band according to Fraser and McRae (1973) as

$$S_v = (E_x^2 - R_{ATR}E_y^2 + E_z^2)/(E_x^2 - R_{ATR}E_y^2 - 2E_z^2) \quad (1)$$

E_x^2, E_y^2, and E_z^2 are the mean square electric fields of the incoming, propagating light wave at the ATR-crystal (Figure 2). For calculating the molecular order parameter from S_v, one has to take into account that in general the spectroscopically detected transition moment **M** is oriented at an angle Θ_M from the molecular director. The distribution of **M** around the average molecular director is characterized by $S_M = \langle 3\cos^2\Theta_M - 1\rangle/2$. Furthermore, the membranes may be not perfectly oriented, which can be described by an orientational order parameter of the mosaic spread, $S_m = \langle 3\cos^2\Theta_m - 1\rangle/2$, assuming the membrane normals to be distributed axial-symmetrically around the laboratory-fixed axis z. With this model, the vibrational order parameter is in fact a product of three different order parameters (Rothschild & Clark, 1979):

$$S_v = S_{mol}S_MS_m \quad (2)$$

In the case of an α-helix, the amide I band appears at around 1657 cm^{-1}. Because vibrational transitions of nonregular (sometimes called random) structures occur in the same wavenumber range (Surewicz & Mantsch, 1988), the dichroic

ratio of the 1657-cm^{-1} feature is actually a superposition of two different bands: that of the α-helix and that of nonregular structures. This has to be taken further into account for the evaluation of the order parameter of an α-helix from the 1657-cm^{-1} band using the relation $R_{ATR} = x_\alpha A_{\parallel\alpha} + (1 - x_\alpha)A_{\parallel U}]/[x_\alpha A_{\perp\alpha} + (1 - x_\alpha)A_{\perp U}]$, where x_α is the fraction of the α-helix band of the 1657-cm^{-1} feature and the indexes α and U correspond to the helix and the unordered components, respectively. The orientational order parameter of the 1657-cm^{-1} band is composed of the orientational order parameter of the α-helix vibration, $S_{v\alpha}$, and that of the nonregular structure transition, S_{vU}, as

$$S_v(1657) = x_\alpha S_{v\alpha} + (1 - x_\alpha)S_{vU}$$
$$S_{v\alpha} = S_\alpha S_{M\alpha} S_m$$
$$S_{vU} = S_U S_{MU} S_m \quad (3)$$

Because by definition $S_{vU} = 0$, eq 1 changes for the α-helix to

$$S_{v\alpha} = (E_x^2 - R_{ATR}E_y^2 + E_z^2)/[x_\alpha(E_x^2 - R_{ATR}E_y^2 - 2E_z^2)] \quad (4)$$

To be able to evaluate the orientational order parameter of the α-helix ($S_{mol} = S_\alpha$), the orientational order parameter of the amide I helix transition moment, $S_{M\alpha}$, with respect to the helix axis has to be known. Two extreme values are reported in the literature with $S_{M\alpha} = 0.41$ (Tsuboi, 1962) and $S_{M\alpha} = 0.60$ (Rothschild & Clark, 1979). The value of Tsuboi refers to crystals of poly(benzylglutamate). The reported $S_{M\alpha}$ of Rothschild and Clark was determined for bacteriorhodopsin in macroscopically oriented multilayers of purple membranes. Here we use neither of the two values, but calculate from the original polarization measurements of Rothschild and Clark (1979) the presently most reliable value of $S_{M\alpha}$ in view of the recently published high-resolution structure of bacteriorhodopsin (Henderson et al., 1990). Applying this three-dimensional structure with the particular tilt angles of the 7 transmembrane helices and the ca. 10 helical residues lying flat on the membrane plane, one calculates an average helix order parameter of bacteriorhodopsin $S_\alpha = 0.83$. Taking this value, together with the experimental value of $S_{v\alpha} = 0.488 \pm 0.06$ (Rothschild & Clark, 1979), one obtains from eq 3 the product $S_{M\alpha}S_m = 0.59 \pm 0.07$. In the context of the present work, we will use this value for the product of the two order parameters to calculate the molecular order parameters of the procoat and coat protein helices. Thereby, we assume that the mosaic spread of our oriented membranes is comparable to that of the purple membranes in the case of Rothschild and Clark (1979).

The mean square electric fields E_x^2, E_y^2, and E_z^2 of the incoming, propagating light wave at the ATR-crystal/lipid/air or ATR-crystal/lipid/water interface can be calculated with the corresponding refractive indexes of Ge ($n = 4.0$), the lipid film ($n = 1.40$), and air ($n = 1.00$) according to the equations given by Fringeli and Günthard (1981): in the amide I band region for the lipid/air interface, $E_x^2 = 1.99$, $E_y^2 = 2.13$, and $E_z^2 = 0.59$, and for the membrane/D_2O interface, $E_x^2 = 1.97$, $E_y^2 = 2.24$, and $E_z^2 = 1.99$.

The 1500–1800-cm^{-1} region of an infrared spectrum was analyzed as a sum of Gaussian/Lorentzian curves. A linear least-squares fit routine was used where consecutively the amplitudes, band positions, half-widths, and Gaussian/Lorentzian composition were optimized. The number and starting positions of each band incorporated in the fit were deduced from second-derivative and deconvoluted spectra.

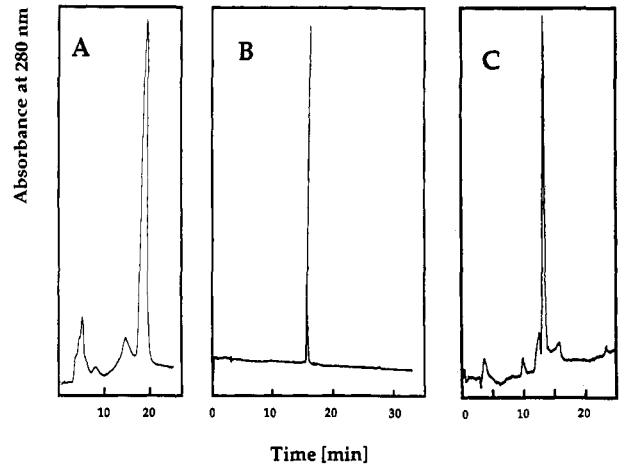

FIGURE 3: HPLC runs of (A) M13 procoat protein, (B) M13 coat protein, and (C) Pf3 coat protein on a C_2 reversed-phase column (125 × 4 mm^2). The proteins were detected at 280 nm and at 214 nm (not shown); 100 μL of a 0.2 mg/mL procoat protein solution (after a first purification step of the raw extract of the *E. coli* membranes on a preparative column) in 2-propanol (0.1% TFA)/water (0.1% TFA), 1/1, 15 μL of a 2.6 mg/mL M13 coat protein solution (extract of phages) in 2-propanol/0.1% TFA, and 20 μL of a 0.1 mg/mL Pf3 coat protein solution (extract of phages) in 2-propanol/0.1% TFA were applied to the column and subsequently eluted with mixtures of 2-propanol/0.1% TFA and water/0.1% TFA under conditions and with compositions of the organic solvent component as follows: (A) 0–4 min 40%, 4–12-min linear gradient 40–48%, 12–20 min 48%, 20–25-min linear gradient 48–100%; (B) 0–10-min linear gradient 35–40%, 10–70-min linear gradient 40–100%; (C) 0–5 min 40%, 5–45-min linear gradient 40–100%.

Spectra of peptide/lipid vesicles in water were acquired using CaF_2 windows with a path length of less than 6 μm. In order to obtain pure protein spectra, the spectra of water and lipids, respectively, were subtracted from the corresponding original spectra. The amide I bands (1600–1700 cm^{-1}) were analyzed against the 12 reference proteins cited above, using a method based on Hennesy and Johnson's procedure described for CD evaluations. The method applied here is comparable with that of Lee et al. (1990), as is the correlation between the protein secondary structures obtained by FTIR and X-ray diffraction.

RESULTS

Protein Purification. Figure 3 shows HPLC runs of M13 procoat, coat, and Pf3 coat proteins according to the procedures described under Materials and Methods. In each case, a major protein peak is recorded, with detection at both 280 nm and 214 nm (not shown), indicating an apparent homogeneous protein preparation with more than 90% purity. Only the volume fractions corresponding to the major protein band were collected and used for the spectroscopic measurements. The minor peak appearing at 15 min in the HPLC run of procoat protein shows the same properties on an SDS gel as the major peak and is therefore assigned as a higher molecular aggregate of the procoat protein in the 2-propanol/water mixture. Whether this aggregate is induced during the HPLC column chromatographic run is not clear at present. Also in the case of the Pf3 coat protein the small bands appearing at 10, 13, and 15 min in the chromatogram of Figure 3C correspond, according to SDS gel electrophoresis, to the same protein as the major HPLC band. Total amino acid analysis and N-terminal sequencing as well as SDS gel electrophoresis have been performed on the protein solutions from the major HPLC bands, and the results obtained confirm a homogeneous preparation of the corresponding proteins. Furthermore, time-

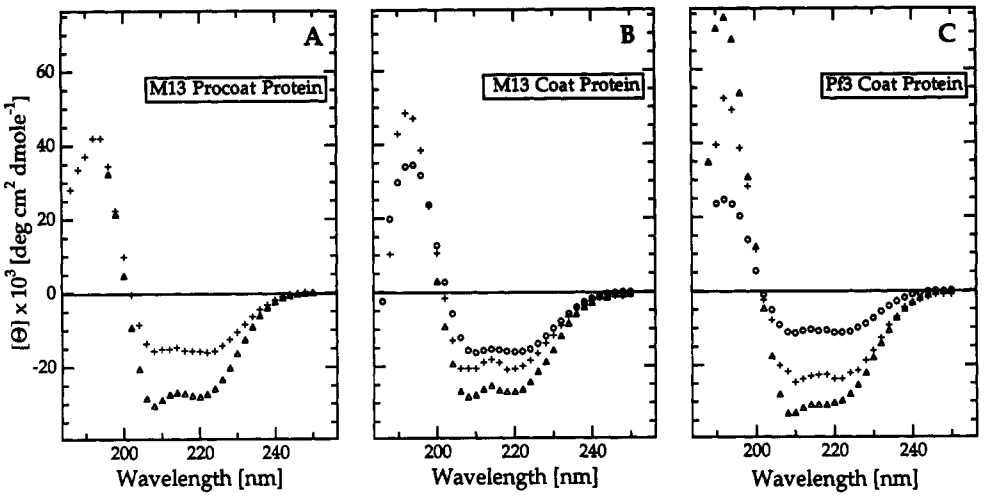

FIGURE 4: CD spectra of (A) M13 procoat protein, (B) M13 coat protein, and (C) Pf3 coat protein, each protein dissolved in 2-propanol (Δ), incorporated in membranes of POPC/POPG lipid vesicles at a lipid to protein molar ratio of 100 in 1 mM Tris-HCl, pH 7.4 (+), and dissolved in buffer (1 mM Tris-HCl, pH 7.4) (○). Protein concentration was 0.1 mg/mL, temperature 25 °C.

resolved measurements of the protein's Trp fluorescence anisotropy yielded rotational correlation times of ϕ = 6–8 ns for M13 procoat, ϕ = 2 ns for M13 coat, and ϕ = 5–6 ns for Pf3 coat proteins in 2-propanol (details will be published elsewhere). This demonstrates that M13 coat protein is dissolved in a monomolecular form, M13 procoat protein as a dimer, and Pf3 coat protein as a trimer in this particular solvent. Similar results were obtained for protein solutions in methanol and ethanol in the presence of 0.1% TFA.

It is interesting to note that the high purify of the M13 procoat protein preparation was obtained by a single extraction of crude *E. coli* membranes with a 1/1 mixture of 2-propanol/formic acid followed by a double HPLC purification step on a C_2 reversed-phase column. In order to obtain a pure preparation of M13 and Pf3 coat proteins, only a single extraction of the corresponding phages by 2-propanol/0.1% TFA was necessary.

Circular Dichroism Measurements. Figure 4A shows the circular dichroism spectra of M13 procoat protein dissolved in 2-propanol/0.1% TFA and incorporated in lipid vesicles of POPC/POPG at a molar ratio of 1/1. In 2-propanol, the average helix content of procoat protein is [α] = 90 ± 5%. Upon incorporation into lipid membranes (mixed film reconstitution method), a considerable decrease of the helix content was observed with [α] = 50%. The helix content for procoat protein in SDS micelles is comparable to that in lipid membranes of POPC/POPG. However, in pure POPC membranes, procoat protein adopts a conformation with a substantially lower helix content, indicating that an electrostatic interaction between procoat protein and the negative membrane surface charges of POPG also plays a role in the formation of the membrane-incorporated protein structure. The secondary structures of the three proteins in the different environments as determined by CD are summarized in Table I.

Figure 4B and Figure 4C show the CD spectra of M13 coat and Pf3 coat proteins, respectively, each in 2-propanol/0.1% TFA, in water, and in lipid membranes (mixed film reconstitution method). The average protein secondary structure for the two coat proteins is [α] = 90 ± 5%, similar to the case of procoat protein. Upon incorporation into lipid vesicles, the α-helix content decreases to [α] = 70% in the case of Pf3 and to [α] = 60% for M13 coat protein. It should be noted that the membrane incorporation of the three different proteins according to the different reconstitution procedures described under Materials and Methods yielded, within experimental error, identical results. As in the case of procoat protein, the

Table I: Helix Content Derived from CD Spectra of the M13 Procoat, M13 Coat, and Pf3 Coat Proteins in Different Environments

	% helix[a]		
sample	M13 procoat	M13 coat	Pf3 coat
2-propanol/0.1% TFA[b]	90	90	90
1 mM Tris-HCl, pH 7.4[b]		50	40
0.5% SDS/ 1 mM Tris-HCl, pH 7.4[c]	45	55	65
1/1 POPC/POPG vesicles[b]	50	60	75
POPC vesicles[c]		45	40

[a] Values are rounded to 5%. Shown are average values of measurements of five different samples. [b] Standard deviation was ±5%. [c] Standard deviation was ±10%.

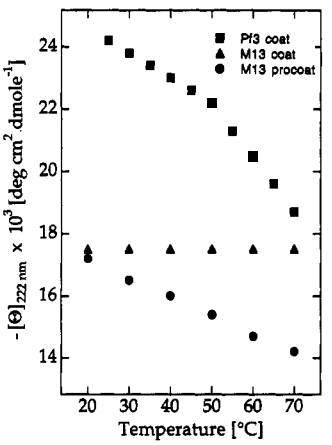

FIGURE 5: Molar ellipticities at 222 nm, [Θ_{222}], of M13 procoat protein (●), M13 coat protein (▲), and Pf3 coat protein (■) at different temperatures. Each protein was incorporated in membranes of POPC/POPG lipid vesicles at a lipid to protein molar ratio of 100. Protein concentration was 1 μM, buffer 1 mM Tris-HCl, pH 7.4, and path length of the optical cell 1 cm.

secondary structure of the two coat proteins in SDS micelles is comparable to that in POPC/POPG membranes. The predominantly α-helical structure is even preserved in an aqueous protein solution with [α] = 40% for Pf3 and [α] = 50% for coat protein. The stability of the secondary structure of the three proteins in lipid membranes was investigated at different temperatures by CD measurements. The mean residual ellipticities at 222 nm, $[\Theta]_{222}$, for the three proteins were measured between 20 and 80 °C as shown in Figure 5. For M13 coat protein, $[\Theta]_{222}$ is constant in the whole investigated temperature range, while for M13 procoat and

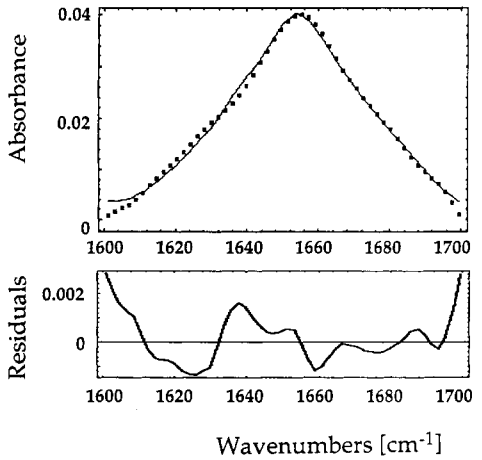

FIGURE 6: FTIR spectrum of the amide I region of M13 coat protein in an aqueous dispersion of POPC/POPG membranes at 25 °C. Molar lipid to protein ratio was 80. Buffer and lipid spectral components were subtracted. Points represent experimental values; the full line corresponds to the fitted spectrum. Residuals were calculated as the difference between the fitted and experimental spectra.

Pf3 coat proteins the $[\Theta]_{222}$ values decrease continuously with increasing temperature. Above 60 °C, samples with procoat protein did not reach a stable CD signal. The $[\Theta]_{222}$ value is, to a good approximation, proportional to the α-helix content of the corresponding protein. According to these experimental results, the α-helical structures of M13 coat protein in lipid membranes are considerably more stable than the corresponding helices of M13 procoat and Pf3 proteins.

FTIR Spectroscopy of M13 Coat Protein in Lipid Vesicles. Figure 6 shows the FTIR spectrum in the amide I band of M13 coat protein in an aqueous dispersion of POPC/POPG vesicles. The maximum of the relatively structureless amide I band at 1655 cm^{-1} indicates a predominantly α-helical secondary structure for the membrane-bound coat protein. Analysis of the amide I band by a fit with reference protein spectra determines the protein secondary structure as 57% α-helix, 13% β-structure, 16% turns, and 14% other. The α-helix content is in excellent agreement with that determined by CD spectroscopy.

ATR–FTIR spectroscopy of Planar Membranes. The orientational order parameters of the different secondary structure elements of the proteins in lipid membranes have been determined by polarized ATR–FTIR measurements. Planar multilayers of protein/lipid membranes were spread on the surface of a Ge ATR-plate, and the infrared spectra were recorded with parallel and perpendicular polarized light, respectively.

Panels A, B, and C of Figure 7 are representative examples of the perpendicular and parallel polarized component spectra (first and second row, respectively) of M13 procoat, M13 coat, and Pf3 coat proteins in planar, air-dried POPC/POPG membranes. In order to resolve the position of the overlapping vibrational components, the second-derivative and deconvoluted spectra are also shown for each particular protein spectrum. Minima in a second-derivative spectrum correspond to maxima or shoulders in the original spectrum.

The amide I bands of the three proteins are similar both in the overall shape as well as in the individual resolved spectral components, which are listed in Table II. Subsequently, the most prominent spectral components were used to fit the parallel and perpendicular polarized FTIR spectra in the 1600–1800-cm^{-1} region, in order to determine the exact values of polarization of the different spectral transitions. The results are included in Figure 7 for the three proteins. Table II summarizes the relevant polarization values for all resolved amide I components of the three different proteins, as well as the corresponding calculated order parameters S_v of the vibrational transitions.

The different bands in the amide I region can be assigned according to numerous published studies (Krimm & Bandekar, 1986; Haris et al., 1986; Byler & Susi, 1986; Surewicz et al., 1987; Surewicz & Mantsch, 1988). The amide I region is dominated by a band at 1657 cm^{-1} which can be assigned to α-helical peptide conformations. However, nonregular structures also appear in the same wavenumber range. The minor bands at 1620 and 1630 cm^{-1} may indicate the presence of β-structures. The small band at 1640 cm^{-1} could be assigned to turns and/or β-structures. The assignment of the bands at 1675 and 1690 cm^{-1} could arise from turns and bends as well as from coupled β-structures. As in the case of CD spectroscopy, different membrane incorporation procedures (see Materials and Methods) yielded practically identical protein IR spectra. However, if the proteins are stored over weeks at room temperature in the 2-propanol/0.1% TFA solution, the membrane incorporation results in a totally different protein conformation, now showing one predominant band at 1630 cm^{-1} (spectrum not shown). Obviously, under this condition, the membrane-incorporated proteins adopt a preferential β-structure. This fact was also reflected in the CD spectra of old protein solutions.

The important finding from the curve fitting in Figure 7 is that the α-helix band at 1657 cm^{-1} is clearly separated from the other spectral features. ATR–FTIR spectra were recorded with membrane preparations of different molar lipid to protein ratios, r. The dichroic ratio of the α-helix band of the three proteins increased with increasing r in the supported lipid membranes, reaching a limiting saturation value at $r = 20$–40 of $R_{ATR} = 1.56$ for M13 procoat protein, $R_{ATR} = 1.71$ for M13 coat protein, and $R_{ATR} = 1.59$ for Pf3 coat protein. Using the relations between R_{ATR}, S_v, and S_α in eq 3 and 4, one calculates the orientational order parameter of the average α-helix axis for procoat protein as $S_\alpha = 0.56$–0.71, for M13 coat protein as $S_\alpha = 0.73$–0.92, and for Pf3 coat protein as $S_\alpha = 0.52$–0.65 (the two values reported in each case are due to the uncertainty of $S_{M\alpha}S_m = 0.52$–0.66 in eq 3; see Materials and Methods for details). This result indicates that the helices are oriented preferentially parallel to the membrane normal.

Upon hydration of the planar membranes with D_2O water/vapor, the amide bond hydrogens which are accessible to water exchange to deuterons. As a consequence, the deuterated peptide bonds exhibit an altered amide I spectrum. This is shown in Figure 8 for the case of M13 coat protein in POPC/POPG membranes. There is no significant difference of the amide I maximum in H_2O (1657 cm^{-1}) and in D_2O (1656 cm^{-1}). Similar observations were made with the M13 procoat and the Pf3 coat proteins in POPC/POPG membranes as well as for the three proteins with bulk D_2O. According to literature values, a totally deuterated α-helix polypeptide backbone, such as in hemoglobin, myoglobin, or cytochrome c, would give rise to an amide I band at 1650–1651 cm^{-1} (Byler & Susi, 1986). The results for the three membrane-incorporated proteins in the present case indicate that the α-helices are not, or only partially, accessible to water within the time range of equilibration (hours). Compared to the amide I band spectra of the H_2O-suspended membranes, dried in air, the spectra of the amide I bands of the D_2O-hydrated membranes show a substantial intensity decrease between 1670 and 1700 cm^{-1} and a concomitant increase in the

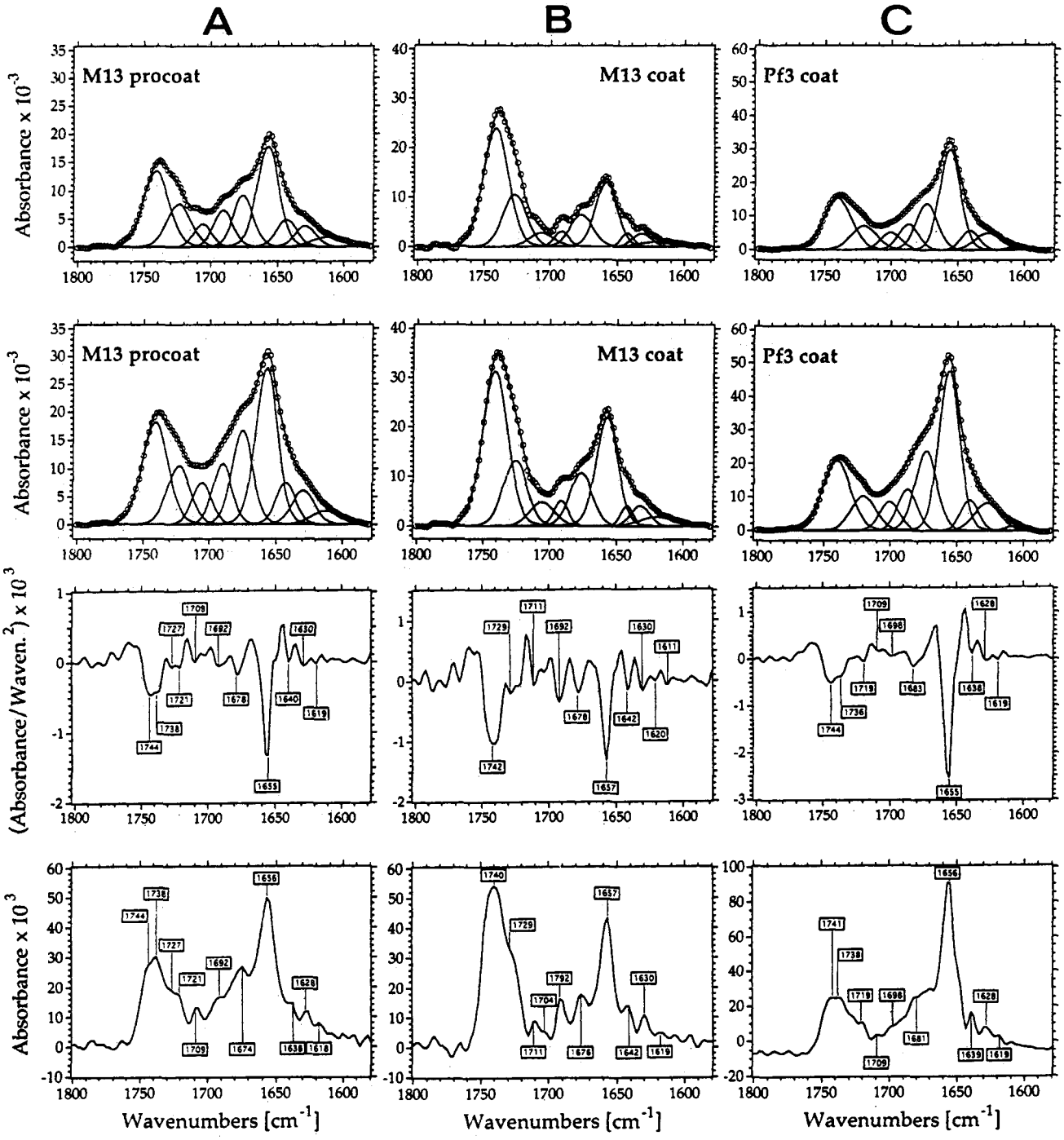

FIGURE 7: ATR–FTIR of air-dried POPC/POPG membranes at 25 °C containing (A) M13 procoat protein at a molar lipid to protein ratio $r = 40$, (B) M13 coat protein at $r = 80$, and (C) Pf3 coat protein at $r = 20$. Shown for each case are the protein spectra for perpendicular polarization (first row, counted from top) and for parallel polarization (second row) together with the best-fitted individual bands. Also the second-derivative (third row) and deconvolution (lowest row) spectra of the parallel polarized protein spectra are shown.

1620–1645-cm^{-1} range. The relative intensity of the band at 1641 cm^{-1} to that at 1656 cm^{-1} is higher in D_2O than in air/H_2O for all three proteins. A similar observation was made by others with water-soluble proteins (Yang et al., 1987). In the case of H_2O-hydrated proteins, the spectral features of the nonregular protein structures appear around 1657 cm^{-1} together with the vibrational bands of an α-helix. When the corresponding peptide bonds are deuterated, the nonregular protein structure bands are shifted toward 1640–1645 cm^{-1} (Byler & Susi, 1986). Therefore, in the deuterated protein spectra of Figure 8, the band observed at 1656 cm^{-1} is a pure "helix" band, free of other structure components. Interestingly, the dichroic ratio is measured to be $R_{ATR} = 1.73$ in the H_2O/air spectra and $R_{ATR} = 1.93$ in the deuterated membranes. This corresponds to nearly identical order parameters of the helix amide I transition moment, namely, $S_{v\alpha} = 0.48$ for H_2O and $S_{v\alpha} = 0.46$ for D_2O.

Due to severe overlap, the dichroic ratios of the other bands in the amide I region are less well-defined than those of the α-helix bands. Small changes in the base line or in the ratio between Gaussian and Lorentzian line shapes in the curve fitting influence the line-shapes of the nonhelix bands more than those of the 1657-cm^{-1} feature. The orientational order parameters of the β-strands as calculated from the dichroic ratios of the β-structure bands at 1620 and 1630 cm^{-1} range between $S_\beta = -0.56$ and -0.70 (Table II). The physically reasonable lower limit of an orientational order parameter is -0.5. In spite of the uncertainties, the determined S_β values

Table II: Assignments, Dichroic Ratios (R_{ATR}), and Concomitant Orientational Order Parameters (S_v) of the Vibrational Transitions of M13 Procoat, M13 Coat, and Pf3 Coat Proteins in POPC/POPG Air-Dried, Supported Planar Lipid Bilayers

band position[a] (cm^{-1})	assignment[b]	R_{ATR}[c] (S_v)[d] M13 procoat	M13 coat	Pf3 coat
1608–1615	β-strand	1.43 (0.21)	1.32 (0.12)	1.79 (0.41)
1628–1631	β-strand	1.63 (0.34)	1.49 (0.25)	1.64 (0.34)
1642–1644	turn/β-strand	1.54 (0.28)	1.50 (0.26)	1.61 (0.32)
1657	α-helix/nonregular	1.56 (0.37)	1.71 (0.47)	1.59 (0.35)
1675–1676	turn/bend	1.83 (0.43)	1.55 (0.29)	1.71 (0.38)
1688–1690	turn/bend	1.67 (0.36)	1.53 (0.28)	1.63 (0.34)
1702–1705	turn/bend	1.84 (0.43)	1.61 (0.32)	1.66 (0.35)
1722–1723	C=O lipid	1.38 (0.17)	1.21 (0)	1.44 (0.22)
1741	C=O lipid	1.36 (0.15)	1.31 (0.11)	1.35 (0.14)

[a] Indicated is the variation of the position of the bands resolved in Figure 7 across the different protein spectra. [b] According to Surewicz and Mantsch (1988) and Byler and Susi (1986) for protein amide I bands, and Blume et al. (1988) for lipid bands. [c] Values calculated from areas of the different band components obtained by fits to the spectra in Figure 7. Typical deviations between R_{ATR} values of different samples at lipid saturation are ±0.02 for the 1657-cm^{-1} band, ±0.07 for the 1608–1615-cm^{-1} band, and ±0.05 for the other features. [d] S_v calculated according to eq 4 for the bands at 1657 cm^{-1} (x_α = 0.8 for M13 procoat and coat proteins and 0.9 for Pf3 coat protein) and according to eq 1 for all other bands.

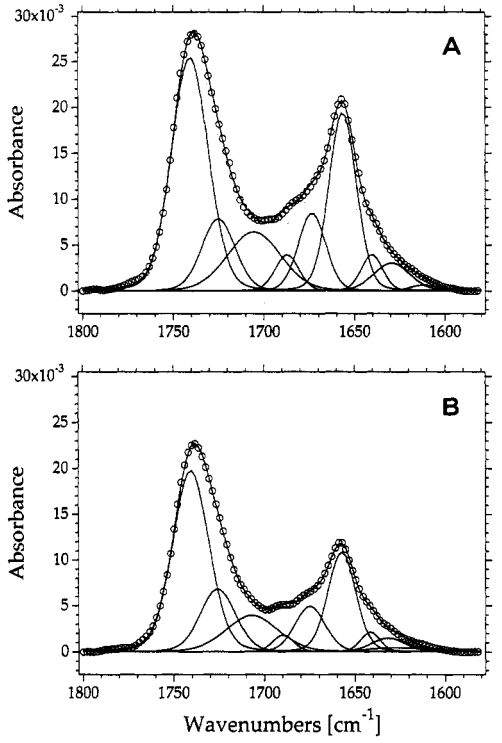

FIGURE 8: Parallel (A) and perpendicular (B) polarized components of the amide I band of M13 coat protein in POPC/POPG membranes after hydration with D_2O vapor at 25 °C together with the best-fitted individual bands.

may indicate that the β-strands of the three membrane-incorporated proteins are oriented parallel to the membrane plane. A similar conclusion can be drawn from the dichroic ratios of the 1675- and 1690-cm^{-1} bands if they indeed correspond to β-structures. If these bands, however, correlate with turn structures, it would be difficult to translate the dichroic ratios to a particular membrane orientation of the turns, because a variety of different turn structures are known, which at present cannot definitely be assigned by the corresponding infrared spectrum.

The vibrational bands at 1722 and 1741 cm^{-1} of the lipid carbonyl bonds in pure planar multibilayers of POPC/POPG show a polarization ratio of R_{ATR} = 1.15 ± 0.05 (spectra not shown) which corresponds to an orientational order parameter of the vibrational transition of S_v = –0.08 ± 0.08. Similar values have been measured by Frey and Tamm (1991) on POPC/POPG multilayers. The values are in agreement with NMR studies of macroscopically aligned multilayers of egg yolk phosphatidylcholine, indicating that the lipid carbonyl groups are oriented close to the "magic angle" of 54.7° with respect to the membrane normal which would yield a value of 0 for the order parameter of the carbonyl groups (Braach-Maskvytis & Cornell, 1988). In the presence of membrane-inserted (pro)coat proteins, the dichroic ratios of the lipid carbonyl bands range from R_{ATR} = 1.21–1.44. The corresponding vibrational order parameters are S_v = 0–0.22.

DISCUSSION

The isolation–purification procedure presented here yields homogeneous preparations of M13 procoat, M13 coat, and Pf3 coat proteins. The method is distinguished by its simplicity and efficacy. Only two purification steps for the procoat protein and only a single extraction in the case of the coat proteins are necessary. Most importantly, the preparation contains proteins in a well-defined structural state. The proteins are dissolved in monomeric (M13 coat), dimeric (M13 procoat), and trimeric form (Pf3 coat) and adopt a nearly totally helical conformation. In this respect, our isolation procedure represents a substantial improvement compared to other published purification protocols for M13 procoat protein (Zwizinski & Wickner, 1982) and M13 coat protein (Knippers & Hoffmann-Berling, 1966; Wickner, 1975; Spruijt et al., 1989). In particular, the published purification methods for M13 coat protein yielded preparations with proteins already aggregated in an undefined and uncontrolled state, as well as produced protein conformations with variable amounts of α-helix and β-strands, depending strongly on the state of aggregation (Spruijt et al., 1989; Spruijt & Hemminga, 1991).

The preparations used in the present work are suited for protein reconstitution and subsequent investigation of the structure and dynamics of the whole membrane insertion and translocation processes *in vitro*. According to the results obtained by CD and FTIR measurements, some general conclusions can be drawn on the structural properties of the three proteins investigated here.

Compared to the nearly totally helical structure in 2-propanol/0.1% TFA, there is a considerable decrease of the helix content when the proteins are incorporated into lipid membranes. Because different membrane reconstitution procedures of the proteins result in nearly identical CD and IR spectra, we assume the presence of a single protein population within the lipid membrane. Hence, according to the data in Table I, the helix structure of membrane-inserted M13 procoat protein is comprised of 37 amino acid residues, that of M13 coat protein 29–31 residues, and that of Pf3 coat protein 33 residues. ATR–FTIR measurements have shown that for all three proteins the helical parts are on average oriented preferentially parallel to the membrane normal, with a substantial higher value of the helix orientational order parameter S_α = 0.81 for M13 coat protein than for M13 procoat and Pf3 coat proteins with S_α = 0.64 and 0.58, respectively. Because the order parameters are derived from ATR–FTIR measurements of air-dried membranes, they reflect primarily the static orientational distribution of the protein helices in a relatively rigid bilayer. Although the polarization measurements in principle do not contain information on the dynamics of protein structure fluctuations, it

is reasonable to expect that in a fluid lipid bilayer the protein helices perform orientational fluctuations around the membrane normal, with internal structural fluctuations within the helix polypeptide backbone superimposed. It was shown elsewhere that for α-helical polypeptides in general and for membrane-inserted helices in particular, such structural fluctuations are largest at the helix ends (Vogel et al., 1988; Daggett & Levitt, 1992). The orientational helix order parameters determined in our case therefore indicate that the mobilities (orientational fluctuations of the whole molecule and/or internal structural fluctuations) of the M13 procoat and Pf3 coat proteins in lipid bilayers are larger than that of the M13 coat protein. This behavior corroborates the observation that the thermal stability of the M13 coat protein is considerably higher than that of M13 procoat protein and Pf3 coat protein in lipid membranes. It is tempting to speculate that the relative high mobility of M13 procoat and Pf3 coat proteins is correlated with their ability to insert spontaneously into membranes within the natural membrane translocation process.

Sanders et al. (1991) performed a molecular dynamics simulation of M13 coat protein monomers and a head to tail dimeric complex in vacuum where the lipid bilayer was taken into account by a hydrophobic potential. During the 100-ps simulation, the nearly totally helical conformation was stable, showing a bend near Gly-38. Furthermore, the largest mobility was observed near the helix ends where the rms fluctuations of the C_α atoms were maximal. Although this study gives interesting information on the relative stability of the helix along the protein sequence, the suggested model has to be revised in view of our present work, which shows that nearly half of the membrane-incorporated protein is nonhelical.

CD and FTIR experiments of the membrane-incorporated proteins reveal the presence of nonhelical structures which could formally be assigned to β-strands and turns. However, the interpretation of the spectra in favor of such structures is not as straightforward and unequivocal as in the case of the helical structures. Whether or not the spectral features, e.g., in the protein FTIR spectra of Figure 7, listed in Table II, are real β-structures or turns is difficult to decide. It is interesting to note in this respect that the FTIR spectra of highly helical proteins, such as hemoglobin, myoglobin, cytochrome *c*, and ferritin, dissolved in D_2O, show amide I bands around 1630 and 1670 cm^{-1} which in principle could be assigned to β-structures (Byler & Susi, 1986). However, because according to X-ray structure analysis neither of these particular proteins shows β-structures in the generally defined sense, those bands have been assigned to the short extended chains connecting the helical segments (Byler & Susi, 1986). For these proteins, the helix-connecting segments consist of two to six residues each, which neither are bent into turns nor form sheets. For comparison, our membrane-inserted (pro)-coat proteins also show bands at 1626 and 1675 cm^{-1} in the deuterated form (Figure 8). Another example is bacteriorhodopsin. Infrared spectra of this intrinsic membrane protein have shown a prominent amide I band at 1660–1663 cm^{-1} representing membrane-spanning helices, as well as bands at 1630–1640 and 1684 cm^{-1} which were assigned to β-structures (Jap et al., 1983; Lee et al., 1985). Obviously, this assignment to β-structures has to be revised, in this particular case, according to the recently published three-dimensional structure of bacteriorhodopsin (Henderson et al., 1990). On the basis of high-resolution electron diffraction experiments, a structural model of bacteriorhodopsin was presented showing a highly helical membrane protein without β-structures. The bands at 1630–1640 and 1684 cm^{-1} observed in the infrared spectra of bacteriorhodopsin therefore likely represent the loop structures connecting the different transmembrane helices. If β-structures are really present in the case of our coat and procoat proteins, they would be oriented preferentially parallel to the membrane plane as indicated by the dichroic ratios of the corresponding bands (Table II). However, the sometimes rather high dichroic ratio of the different nonhelical amide I bands and the concomitant unrealistically low orientational order parameters of the putative β-strands (S_β range from –0.55 to –0.7) argue against a classical β-structure.

Even in aqueous solution, the (pro)coat proteins form a preferential α-helix conformation. Time-resolved fluorescence anisotropy measurements have been performed on these preparations (unpublished results) showing that the proteins form low molecular aggregates composed of about 10 monomers in a buffer of low ionic strength. These low molecular aggregates show a tendency to form higher molecular aggregates within several hours. The time course of the second aggregation step is faster in buffer solutions of high ionic strength. The formation of a water-soluble form of M13 coat protein was recently reported by Spruijt and Hemminga (1991).

The following question arises: How can these results be translated into a molecular model of the membrane-inserted proteins? Biological studies have shown that both M13 and Pf3 coat proteins span the biological membrane after the membrane insertion process (Kuhn & Troschel, 1992). The presently available structural data of membrane proteins indicate that the membrane-traversing protein segments which are in contact with the hydrophobic part of a lipid bilayer fold in general as α-helices or β-strands, in order to saturate hydrogen bonds (Deisenhofer et al., 1985; Henderson et al., 1990; Weiss et al., 1991; Cowan et al., 1992; Vogel, 1992). In the case of the investigated coat proteins, it is reasonable to assume that the central hydrophobic parts traverse the lipid bilayer as an α-helix. This would also explain the low accessibility for water of the M13 coat protein helices in POPC/POPG membranes as measured by FTIR with H_2O–D_2O exchange experiments. Our results are supported by NMR hydrogen exchange measurements on SDS-solubilized M13 coat protein. There the highest exchange rates were measured at the N- and C-termini, while the lowest exchange rates were found for the central hydrophobic segment of the M13 coat protein (Molday et al., 1972). Whether the predicted transmembrane helix extends in the form of a single helix over 30 or 33 amino acid residues for M13 coat and Pf3 coat proteins, respectively, cannot be decided from our spectral data. Our model of the structure of the membrane-inserted coat proteins is in agreement with a recently published model of the M13 coat protein in SDS micelles derived from NMR measurements (Henry & Sykes, 1990).

In the case of a structural model of membrane-inserted M13 procoat protein, similar argumens hold as in the case of the two coat proteins. Biological studies indicate that the procoat protein inserts into membranes in the form of a loop structure between the N- and C-termini located in the cytoplasm (Kuhn, 1987). Because the ATR–FTIR experiments have shown that β-structures, if really present, would be oriented parallel to the membrane plane, the only candidates for the membrane-spanning protein parts are the α-helical segments. Due to the loop structure, at least two helix segments must exist in a procoat molecule, most reasonably the hydrophobic segments in the leader and in the mature coat sequence (Figure 1). The number of 37 amino acid residues

in a procoat molecule, which according to CD spectra form the helical part, fits nicely to this idea. As a consequence of this model, the helical parts in M13 coat protein extend differently than the helical part of the coat sequence in procoat protein.

The data presented in this work cannot distinguish whether the (pro)coat protein molecules are incorporated in a vectorial or in an antiparallel configuration into the lipid bilayer. Our data on the structures of M13 procoat and Pf3 coat proteins are the first in this field. On the other hand, the investigations presented in this work have clarified the long dispute on the helix structure of M13 coat protein in lipid membranes; the published data range from 50 to 90% α-helix content (Nozaki et al., 1976; Fodor et al., 1981; Shon et al., 1991). It is quite interesting to compare our structural data with the recently published three-dimensional structure at 7-Å resolution of the closely related filamentous bacteriophages Pf1 and M13. In the case of Pf1, the coat protein consists of a pair of α-helical segments interrupted by a nonhelical surface loop. The two α-helices appear to be hydrogen-bonded at adjacent ends, thus forming a single, slowly-curving α-helix structure (Nambudripad et al., 1991). The structure of the M13 coat protein in the phage is similar, but formed of a single, gently-curving α-helix, extending from Pro-6 to the carboxy terminus (Glucksman et al., 1992). The flexible portion there is located at the first five residues at the N-terminus. Clearly, in view of our results, the membrane structure of M13 coat protein and of Pf3 coat protein deviates considerably from the form present in phages. The membrane structure appears to be much more disordered and consequently more flexible.

ACKNOWLEDGMENT

We are greatly indebted to P. Infelta for help in the development of various computer programs and to D. Fraser for reading the manuscript.

REFERENCES

Blume, A., Hübner, W., & Messner, G. (1988) *Biochemistry 27*, 8239–8249.

Braach-Makvytis, V. L. B., & Cornell, B. A. (1988) *Biophys. J. 53*, 839–843.

Byler, D. M., & Susi, H. (1986) *Biopolymers 25*, 469–487.

Cornell, D. G., Dluhy, R. A., Briggs, M. S., McKnight, C. J., & Gierasch, L. M. (1989) *Biochemistry 28*, 2789–2797.

Cowan, S. W., Schirmer, T., Rummel, G., Steiert, M., Ghosh, R., Paupit, R. A., Jansonius, J. N., & Rosenbusch, J. P. (1992) *Nature 358*, 727–733.

Daggett, V., & Levitt, M. (1992) *J. Mol. Biol. 223*, 1121–1138.

Deisenhofer, J., Epp, O., Miki, K., Huber, R., & Michel, H. (1985) *Nature 318*, 618–624.

Fodor, S. P. A., Dunker, A. K., Ng, Y. C., Carsten, D., & Williams, R. W. (1981) in *Bacteriophage Assembly*, pp 441–455, Alan Liss Inc., New York.

Fraser, R. D. B., & MacRae, T. P. (1973) *Conformation in Fibrous Proteins and Related Synthetic Peptides*, Academic Press, New York.

Frey, S., & Tamm, L. (1991) *Biophys. J. 60*, 922–930.

Fringeli, U. P., & Günthard, H. H. (1981) in *Membrane Spectroscopy* (Grell, E., Ed.) pp 270–332, Springer Verlag, Berlin.

Fringeli, U. P., Leutert, P., Thurnhofer, H., Fringeli, M., & Burger, M. M. (1986) *Proc. Natl. Acad. Sci. U.S.A. 83*, 1315–1319.

Fürste, J. P., Pansegran, W., Frank, R., Blocker, H., Scholz, P., Bagdasarion, M., Lanka, E. (1986) *Gene 48*, 119–131.

Gallusser, A., & Kuhn, A. (1990) *EMBO J. 9*, 2723–2729.

Geller, B. L., & Wickner, W. (1985) *J. Biol. Chem. 260*, 13281–13285.

Glucksman, M. J., Bhattacharjee, S., & Makowski, L. (1992) *J. Mol. Biol. 226*, 455–470.

Gremlich, H. U., Fringeli, U. P., & Schwyzer, R. (1983) *Biochemistry 22*, 4257–4263.

Haris, I. P., Hayward, J. A., Restall, C. J., & Chapman, D. (1985) *Biochemistry 24*, 4364–4373.

Haris, I. P., Lee, D. C., & Chapman, D. (1986) *Biochim. Biophys. Acta 874*, 255–265.

Henderson, R., Baldwin, J. M., Ceska, T. A., Zemlin, F., Beckmann, E., & Downing, K. H. (1990) *J. Mol. Biol. 213*, 899–929.

Hennesey, J. P., & Johnson, W. C., Jr. (1981) *Biochemistry 20*, 1085–1094.

Henry, G. D., & Sykes, B. D. (1990) *Biochem. Cell Biol. 68*, 318–329.

Ito, K., Date, T., & Wickner, W. (1980) *J. Biol. Chem. 255*, 2123–2130.

Jap, B. K., Maestre, M. F., Hayward, S. B., & Glaeser, R. M. (1983) *Biophys. J. 43*, 81–89.

Kleffel, B., Garavito, R. M., Baumeister, W., & Rosenbusch, J. P. (1985) *EMBO J. 4*, 1589–1592.

Knippers, R., & Hoffmann-Berling, H. (1966) *J. Mol. Biol. 21*, 281–292.

Krimm, S., & Bandekar, J. (1986) *Adv. Protein Chem. 38*, 181–364.

Kuhn, A. (1987) *Science 238*, 1413–1415.

Kuhn, A., & Wickner, W. (1985) *J. Biol. Chem. 260*, 15914–15918.

Kuhn, A., & Troschel, D. (1992) in *Membrane Biogenesis and Protein Targeting* (Neupert, W., & Lill, R., Eds.) pp 33–47, Elsevier, New York.

Kuhn, A., Wickner, W., & Kreil, G. (1986) *Nature 322*, 335–339.

Kuhn, A., Zhu, H.-Y., & Dalbey, R. E. (1990) *EMBO J. 9*, 2385–2388.

Kuhn, A., Gallusser, A., & Rohrer, J. (1992) *J. Struct. Biol. 104*, 38–43.

Lee, D. C., Hayward, J. A., Restall, C. J., & Chapman, D. (1985) *Biochemistry 24*, 4364–4373.

Lee, D. C., Haris, P. I., Chapman, D., & Mitchell, R. C. (1990) *Biochemistry 29*, 9185–9193.

Molday, R. S., Englander, S. W., & Kallen, R. G. (1972) *Biochemistry 11*, 150–159.

Nambudripad, R., Stark, W., & Makowski, L. (1991) *J. Mol. Biol. 220*, 359–379.

Nunari, J., & Walter, P. (1992) *Curr. Opin. Cell Biol. 4*, 573–580.

Nozaki, Y., Chamberlain, B. K., Webster, R. E., & Tanford, C. (1976) *Nature 259*, 335–337.

Ohno-Iwashita, Y., & Wickner, B. (1983) *J. Biol. Chem. 258*, 1895–1900.

Rapoport, T. A. (1992) *Science 258*, 931–936.

Rohrer, J., & Kuhn, A. (1990) *Science 250*, 1418–1421.

Rothschild, K. J., & Clark, N. A. (1979) *Biophys. J. 25*, 473–488.

Sanders, J. C., Nuland, N. A. J., Edholm, O., & Hemminga, M. (1991) *Biophys. Chem. 41*, 193–202.

Shon, K. J., Kim, Y., Colnago, L. A., & Opella, S. J. (1991) *Science 252*, 1303–1305.

Spruijt, R. B., & Hemminga, M. A. (1991) *Biochemistry 30*, 11147–11154.

Spruijt, R. B., Wolfs, C. J. A., & Hemminga, M. A. (1989) *Biochemistry 28*, 9158–9165.

Surewicz, W. K., & Mantsch, H. H. (1988) *Biochim. Biophys. Acta 952*, 115–130.

Surewicz, W. K., Moscarello, M. A., & Mantsch, H. H. (1987) *J. Biol. Chem. 262*, 8598–8602.

Thomas, G. J., Jr., & Day, L. A. (1981) *Proc. Natl. Acad. Sci. U.S.A. 78*, 2962–2966.

Tsuboi, M. (1962) *J. Polym. Sci. 59*, 139–153.

Vogel, H. (1987) *Biochemistry 26*, 4562–4572.
Vogel, H. (1992) *Q. Rev. Biophys. 25*, 433–457.
Vogel, H., Jähnig, F., Hoffmann, V., & Stümpel, J. (1983) *Biochim. Biophys. Acta 733*, 201–209.
Vogel, H., Nilsson, L., Rigler, R., Voges, K. P., & Jung, G. (1988) *Proc. Natl. Acad. Sci. U.S.A. 85*, 5076–5071.
Weiss, M. S., Kreusch, A., Schiltz, E., Nestel, U., Welte, W., Weckesser, I., & Schultz, G. E. (1991) *FEBS Lett. 280*, 379–382.
Wickner, W. (1975) *Proc. Natl. Acad. Sci. U.S.A. 72*, 4749–4753.
Wickner, W. (1988) *Biochemistry 27*, 1081–1086.
Wiech, W., Sagstetter, M., Müller, G., & Zimmermann, R. (1987) *EMBO J. 6*, 1011–1016.
Williams, R. W. (1983) *J. Mol. Biol. 166*, 581–603.
Wolfe, P. B., Rice, M., & Wickner, W. (1985) *J. Biol. Chem. 260*, 1836–1841.
Yang, P. W., Mantsch, H. H., Arrondo, J. L. R., Saint-Girons, I., Guillou, Y., Cohen, G. N., & Bârzu, O. (1987) *Biochemistry 26*, 2706–2711.
Zwizinski, C., & Wickner, W. (1982) *EMBO J. 1*, 573–578.